JACS
JOURNAL OF THE AMERICAN CHEMICAL SOCIETY

COMMUNICATION

pubs.acs.org/JACS

α-$Na_3M_2(PO_4)_3$ (M = Ti, Fe): Absolute Cationic Ordering in NASICON-Type Phases

Houria Kabbour,[†] Daniel Coillot,[†] Marie Colmont,[†] Christian Masquelier,[‡] and Olivier Mentré*[,†]

[†]Unité de Catalyse et de Chimie du Solide, UCCS, CNRS UMR8181, Université Lille Nord de France, 59655 Villeneuve d'Ascq, France
[‡]Laboratoire de Réactivité et de Chimie des Solides, CNRS-Université de Picardie Jules Vernes, 80039 Amiens cedex 1, France

Supporting Information

ABSTRACT: The structure of the fully ordered α-$Na_3Ti_2(PO_4)_3$ NASICON compound was elucidated using high-quality single-crystal data. The cation/vacancy distribution forms a homogeneous 3D arrangement and could represent the absolute cationic ordering available in the full $Na_3M_2(PO_4)_3$ series, as verified for M = Fe. For M = Ti, the reversible α → γ transition was observed at 85 °C, leading to the standard disordered $R\bar{3}c$ γ model. Through JPDF analysis, the most probable Na^+ zigzag M(2)−M(1) diffusion scheme was directly deduced using our accurate crystallographic data.

Since the discovery of superionic conduction in the NASICON-type framework, numerous studies have been and continue to be carried out to explore their attractive properties for a variety of applications such as membranes, gas sensors, electrode and/or solid electrolyte materials for Li or Na batteries, etc. The well-known NASICON skeleton is formed from corner-sharing XO_4 tetrahedra and MO_6 octahedra that create the so-called lantern units, which are assembled into a 3D $M_2X_3O_{12}$ framework that defines M(1) (one position per formula unit) and M(2) (three positions per formula unit) interstitial sites in the rhombohedral form that are usually filled (fully or partially) by mobile alkali ions (A = Li, Na). $A_xM_2(XO_4)_3$ compounds display multiple possibilities for the occupancy of the interstitial sites.[1−3] If one focuses on the topical A = Na, x = 3 case, it appears that the distribution of A in the structure [full occupation of the M(1) and M(2) sites corresponds to x = 4] has been the subject of intensive discussion and is still not resolved in most of the concerned phases. As a rule, the fully ordered (distorted) α phases undergo structural transitions to $R\bar{3}c$ symmetry (γ phase) directly or through an intermediate β structure upon heating, as reported for $Na_3Fe_2(PO_4)_3$.[4] Indeed, to our knowledge, only two models for fully ordered Na^+ cations in the α-NASICON framework have been developed to date on the basis of experimental data:

From single-crystal X-ray diffraction (XRD) data, α-$Na_3Sc_2(PO_4)_3$ was assigned to the "supercell 1" monoclinic space group Cc (a_m, b_m, c_m), which is related to the trigonal lattice (a_h, b_h, c_h) by the relations $a_h = {}^1/_2a_m + {}^1/_2b_m$, $b_h = -{}^1/_2a_m + {}^1/_2b_m$, and $c_h = a_m + 3c_m$.[5] In addition, Sotofte and Fu[6] debated the low-temperature symmetry and came to the conclusion that α-$Na_3Sc_2(PO_4)_3$ crystallizes in $R\bar{3}c$ (i.e., similar to the γ phase). However, it is remarkable that several other low-temperature structure models that have been refined have led to structural changes depending on the sample preparation, so one cannot state an absolute ordering. Despite inaccurate or misconceived analysis due to the poor data quality, the metastable cationic distribution stabilized at room temperature appears to be strongly dependent on the synthesis route and the size of the crystallite.[7]

A fully ordered model of $Na_3Fe_2(PO_4)_3$ was proposed on the basis of powder neutron diffraction (PND) data (supercell 1, $C2/c$),[8] but short Na−O distances of 1.9 Å dismissed its pertinence. In addition, it was reconsidered later on the basis of extra peaks in the powder XRD pattern, leading to the proposal of "supercell 2" with the space group $C2/c$, which is obtained by the relations $a_m = a_h + 2b_h$, $b_m = -a_h$, and $c_m = c_h$.[3] To the best of our knowledge, the structure has not been solved in this unit cell.

Hence, there is not still a consensus about a total cationic order over the M(1) and M(2) sites, while the possibility of a unified, thermodynamically stable model is attractive. In fact, according to the minor changes in the simulated PND and XRD patterns of antagonist models, high-quality single-crystal data are necessary to probe the Na^+ sublattice correctly. In addition, a proper treatment of twin domains involved in subsymmetry polymorphs appears to be of real importance for this system.

Among the concerned series, $Na_3Ti_2(PO_4)_3$ has been the subject of prior structural[9] and electrochemical[10] characterizations on powder samples; meanwhile, the only structure brought into view at room temperature is of the γ type. We tackled the growth of high-quality single crystals of this phase for the investigation of phase transitions between related forms, bypassing powder obstacles and twin misconceptions to reach the absolute Na^+ ordering of the α-phase. The single crystals were obtained through a multistep solid-state synthesis procedure from a mixture of Na_2CO_3, TiO_2, and $(NH_4)_2HPO_4$ in a stoichiometric ratio. After 3 days in air at 500 °C, the intermediate product was held under reducing conditions (3% H_2 in a N_2 gas flow) at 900 °C for 48 h in a gold crucible. The reduced sample was finally cooled using a ramp of 5 °C/h from 900 to 700 °C and then a ramp of 15 °C/h from 700 °C to room temperature, leading to the isolation of pale-blue single crystals.

XRD intensities were collected on a Bruker SMART CCD-1K diffractometer (Mo Kα radiation, λ = 0.7173 Å) and then integrated and corrected for Lorentz polarization, background, and absorption effects using *SAINT*[11] and *SADABS*.[12] The crystal structures were refined using the *JANA2000* suite.[13] The XRD data analysis revealed weak spots violating the $-h + k + l = 3n$ (obverse) and $h - k + l = 3n$ (reverse) R lattice conditions, and a superstructure of the γ form ($R\bar{3}c$) appeared to be most conclusive. The crystal structure refinement using only

Received: May 18, 2011
Published: July 01, 2011

 © 2011 American Chemical Society

Table 1. Single-Crystal XRD Refinements for the RT Phase of $Na_3Ti_2(PO_4)_3$ in Different Space Groups[a]

	$R\bar{3}c$	$C2/c$	Cc	$C2$	$P\bar{1}$
a (Å)	8.8706(5)	15.3649(9)	15.3649(9)	15.3649(9)	8.8623(6)
b (Å)		8.8622(6)	8.8622(6)	8.8622(6)	8.8693(5)
c (Å)	21.6556(14)	21.6428(13)	21.6428(13)	21.6428(13)	21.6431(13)
angles (deg)		β = 90.066(4)	β = 90.066(4)	β = 90.066(4)	α = 90.066(3), β = 89.973(3), γ = 119.982(3)
indep reflns [$I > 3\sigma(I)$]	447/339	5216/3492	9237/5821	8952/5691	8938/5640
R_{obs}/wR_{obs}	3.20/3.55	12.88/12.32	3.74/3.52	4.12/3.91	3.34/3.14*; 3.74/3.54**
parameters	37	186	362	364	547*; 372**
weighting scheme	$1/\sigma^2$	unit	unit	unit	unit
max/min $\Delta\rho$ (e/Å^3)	0.43/−0.26	7.45/−2.58	0.50/−0.49	1.34/−1.34	0.41/−0.38
twinning	hkl − 180°/c	hkl − 120° − 240°/c	hkl − 120° − 240°/c	hkl − 120° − 240°/c	hkl − 120° − 240°/c
twinning ratio	97(1)/3(1)	36(1)/32(1)/31(1)	60.0(4)/20.1(3)/20.3(3)	19.2(4)/41.7(3)/38.9(3)	58.9(4)/19.7(3)/21.2(3)
Ti	12c	3 × 8f	6 × 4a	6 × 4c	6 × 2i
P	18c	4e + 4 × 8f	9 × 4a	2a + 2b + 8 × 4a	9 × 2i
O	2 × 36f	18 × 8f	36 × 4a	36 × 4c	36 × 2i
sites M(1)	6b	4a + 8f	3 × 4a	3 × 4c	1a + 1b + 2 × 2i
sites M(2)	18e, 68(1)%[b]	3 × 8f[c]	6 × 4a[d]	6 × 4c[e]	6 × 2i[f]

[a] Twinning matrices are given in the SI. [b] All atoms set anisotropic. M(1) fully occupied and M(2) partially occupied ($\sim^2/_3$). [c] 2Ti, 5P, 3Na not positive-definite. O set isotropic, otherwise not all positive-definite. M(1) and M(2) fully occupied. [d] Ti, Na, P anisotropic. O set isotropic, otherwise not all positive-definite. M(1) and M(2) fully occupied. [e] Ti, Na, P anisotropic. O set isotropic, otherwise not all positive-definite. M(1) and M(2) fully occupied. [f] * = O anisotropic. ** = O isotropic. M(1) and M(2) occupancies spontaneously converged to 1.

fundamental reflections confirmed the parent $Na_3Ti_2(PO_4)_3$ γ phase [occupancies: M(1), 100%; M(2), 66%]. In trigonal symmetry, our analysis confirmed the nearly single orientation of our sample [obverse/reverse twinning ratio of 97(1)/3(1)], which was helpful in investigating the supercell ordering. In fact, on the basis of the full data set, a fully ordered Na^+ model was reached in the $P\bar{1}$ space group after the introduction of twinning due to the loss of the threefold axis. It spontaneously converged to a structure having two-thirds of the M(2)-related sites filled and one-third empty, with excellent R factors (see Table 1).

Following the group−subgroup relationships, we built a Bärnighausen tree that highlights the path from the high-temperature symmetry to possible low-temperature reduced symmetries [see the Supporting Information (SI)]. The examination of the Na^+ ordering over the M(2) sites excluded the conservation of the trigonal symmetry, as experimentally verified by our partially disordered refinements in the permitted space groups $P\bar{3}c1$, $P3c1$, $P3_121$, etc., all of which led to discrepancies in the thermal parameters. We also examined other models suggested in the literature, such as supercell 1 [a = 15.3581(5) Å, b = 8.8670(13) Å, c = 8.8464(13) Å, β = 125.359°], which did not include most of the supercell spots. In fact, our triclinic Na^+ distribution is fully compatible with monoclinic supercell 2 (see above), as suggested by Masquelier et al.[3] and d'Yvoire and co-workers[4] for the α-$Na_3Fe_2(PO_4)_3$ phase. Despite the possibility of describing the expected cationic ordering in space groups $C2/c$ (R_1 = 12.88%), Cc (R_1 = 3.74%), and $C2$ (R_1 = 4.12%), the examination of the reliability factors together with the anisotropic thermal displacements pointed unambiguously toward $P\bar{1}$ as the most relevant symmetry for α-$Na_3Ti_2(PO_4)_3$ (Figure 1). It is noteworthy that only this choice yielded reasonable anisotropic thermal parameters for all of the atoms without any restraints. However, the similarity with the tested monoclinic model argued for a pseudo-$C2/c$ symmetry. The comparison of the various refinements is presented in Table 1.

The octahedral Ti−O distances for the six independent Ti atoms are 1.95−2.12 Å, leading to bond valence sums in excellent agreement with the trivalent state for Ti ($3.04 < S < 3.07$). In $P\bar{1}$ symmetry, the fully occupied sites Na(1a−d) correspond to the M(1) sites, while the fully occupied Na(2a−f) sites relate to two-thirds of the available M(2) sites. In Figure 2, the Na(2)/□ ordering is shown on planes parallel to $(1\bar{1}0)$ (Figure 2c). The filled and empty sites are ordered along diagonal rows according to the sequence ...□−□−Na(2)−Na(2)−Na(2)−Na(2)..., these rows being shifted along c. The 2D observation of these diffusion paths is somewhat misleading, since crossroads exist at each M(1) site because of the pseudo-threefold axis, leading to a 3D diffusion network (Figure 1). Strikingly, Na(2) positions are more or less displaced off the center of their ideal O_6 antiprism depending on the presence or absence of sodium in the next M(2) site. Typically we found distorted Na(1b) /Na(1c) antiprisms with 2.31 Å < d_{Na-O} < 2.78 Å and regular Na(1a)/Na(1d) antiprisms (2.44 Å < d_{Na-O} < 2.50 Å). In the γ "disordered" type, each M(1) site is surrounded by six M(2) sites statistically two-thirds occupied, while in the α phase, each Na(1) site is surrounded by four fully occupied Na(2) sites and two vacant positions. However, two different Na(1)−[Na(2)$_4$□$_2$] topologies cohabit (Figure 2a). A comparison of the Na(2)/□ arrangements in α-$Na_3Ti_2(PO_4)_3$ and the proposed model for α-$Na_3Sc_2(PO_4)_3$ (monoclinic space group Cc)[7] is shown in Figure 2b,c. Na(2) sites form honeycombs centered by vacancies arranged in layers. In our model, six layers perpendicular to the pseudo-threefold axis are necessary to define the full period, while four layers were used for the scandium compound, leading to only one type of Na(1)[Na(2)$_4$□$_2$]. As already noted, the literature for the latter is contradictory, and the monoclinic distortion has been

dx.doi.org/10.1021/ja204321y |J. Am. Chem. Soc. 2011, 133, 11900–11903

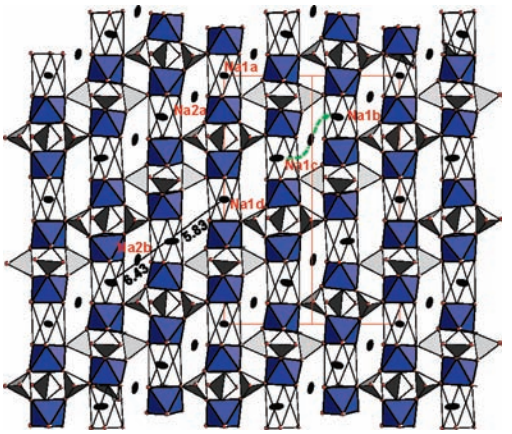

Figure 1. 2D portion of α-$Na_3Ti_2P_3O_{12}$ structure with the Na2/□ scheme. Black ellipsoids represent Na atoms. Transparent antiprisms represent Na in M1 sites. One diffusion path is shown in green. M1−M1 distances across filled and empty M2 sites are indicated.

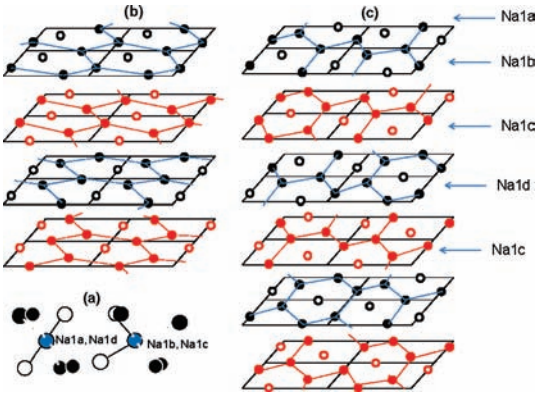

Figure 2. (a)[M1/M2$_4$□$_2$] units in α-$Na_3Ti_2P_3O_{12}$. Black solid spheres represent Na2 atoms. Open spheres are vacant. Na2/□ order in (b) α-$Na_3Sc_2P_3O_{12}$ (ref 6) and (c) in α-$Na_3Ti_2P_3O_{12}$ along (1−10) planes. The unit cell is shifted to compare with (b).

disregarded in later works. The most questionable point concerns the displacement of both Na(1) and Na(2) cations far from their ideal positions as shown in Figure 2c [typically Na(1) is displaced at the center of an O_4 face], contrary to all other reports. Without refuting the validity of prior work on α-$Na_3Sc_2(PO_4)_3$, we can at least endow it with a particular role in the $Na_3M_2(PO_4)_3$ series.

Hitherto and to the best of our knowledge, the vacancy scheme exhibited by α-$Na_3Ti_2(PO_4)_3$ is unique. It reflects a much more homogeneous distribution of intra- and interlayer vacancies, which favor a greater thermodynamic stability potentially extendable to most of the $Na_3M_2(PO_4)_3$ compounds. It was verified using room-temperature PND (λ = 1.22 Å, 3T2, LLB, Saclay, France) that this same model is also applicable to α-$Na_3Fe_2(PO_4)_3$, which is stable for T < 95 °C.[14] Having already pointed out the limitation of powder diffraction data in probing such a sodium ordering within the heavy $M_2(PO_4)_3$ framework, however, we note that our preferred cationic arrangement adapted to its ideal monoclinic $C2/c$ symmetry leads to the best refinements (R_{Bragg} = 2.85%, R_F = 2.05%) among many models tested. Moreover, in view of the poor contribution of Na in PND patterns and the rather good convergence for all of the tested models (see the SI), we

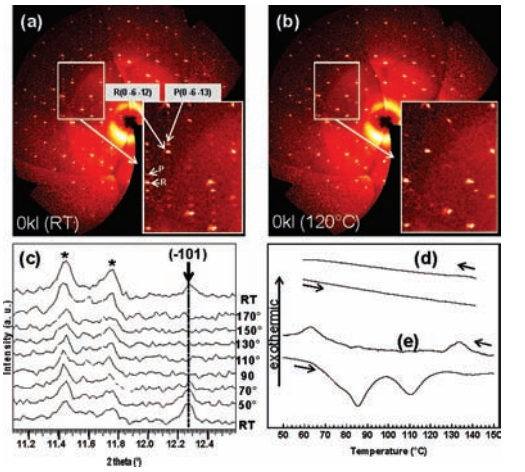

Figure 3. (0kl) layer at (a) 25 °C and (b) 120 °C with evidence of main (R) and primitives (P) reflections. (c) HTXRD showing the evolution of a P line. The stars show impurities peaks of $Na_4(TiO)(PO_4)_2$. (d) DSC of $NaTi_2P_3O_{12}$ and (e) of our preparation.

checked that the refined α-$Fe_2(PO_4)_3$ lattice showed local distortion adapted to the expected presence or absence of Na in the M(2) sites, as in our refined model for the Ti compound. Consequently, the complete and original order of the sodium ions evidenced here for M = Ti, Fe may pave the way to other NASICON compositions with undefined low-temperature structures.

For M = Ti, a transition into the γ phase was expected upon heating, as confirmed by temperature-controlled microsource XRD experiments. A single crystal fixed with Araldite on a glass fiber could be analyzed at 120 °C without degradation.

The precession images emphasize the reversible $\alpha_{(\text{pseudo-}C2/c)} \rightleftarrows \gamma_{(R\bar{3}c)}$ transition for $Na_3Ti_2(PO_4)_3$ as depicted in Figure 3, with reversible extinctions of the primitive reflections in the 0kl layer upon heating/cooling. This transition was located at 85 °C by differential scanning calorimetry (DSC) analysis of the parent sample. After the sample was crushed, four phases were identified by powder XRD: $Na_4(TiO)(PO_4)_2$,[15] $NaTi_2(PO_4)_3$ [a = 8.469(1) Å, c = 21.761(2) Å],[16] α-$Na_3Ti_2(PO_4)_3$ [a = 8.836(1) Å, c = 21.606(2) Å], and a fourth phase assigned as α-$Na_{3-x}Ti_2(PO_4)_3$ [a = 8.811(1) Å, c = 21.689(2) Å]. Two reversible endothermic peaks at 85 and 112 °C appeared upon heating and shifted somewhat (to 62 and 136 °C, respectively) upon cooling (Figure 3e). These correspond to order−disorder transitions for the two α forms. A signature from $NaTi_2(PO_4)_3$ was excluded, giving rise to a flat DSC curve (Figure 3d), and $Na_4(TiO)(PO_4)_2$ has been reported to sustain a transition above ∼350 °C.[17] Therefore, high-temperature powder XRD experiments on a ground sample of the preparation were carried out in the low-2θ region, where additional primitive reflections were present at room temperature: (100) at 11.52°, which was hidden by two broad peaks from $Na_4(TiO)(PO_4)_2$, and ($\bar{1}$01) at 12.22°. The latter reflection appeared as a unique well-defined peak and thus represents a good indicator. As shown in Figure 3c, it disappeared above 70 °C, comfirming the α → γ transition. Finally, it reappeared upon cooling, demonstrating the reversibility of the order−disorder transition. Although a displacive second-order transition is likely because of the cationic sublattice ordering only, the abrupt transition from $R\bar{3}c$ to $P\bar{1}$ rather supports a first-order transition type. In addition, the peaks observed by DSC and the hysteresis upon heating and cooling further support this hypothesis.[18]

dx.doi.org/10.1021/ja204321y |J. Am. Chem. Soc. 2011, 133, 11900–11903

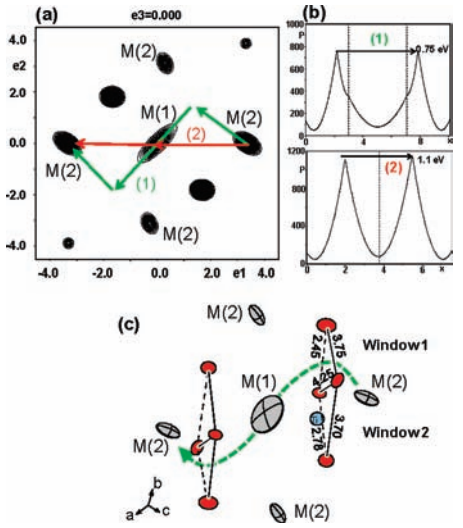

Figure 4. (a) JPDF and (b) energy barriers for paths 1 and 2. (c) Path 1 is preferred for Na diffusion (green path).

Contrary to powder XRD data, the single-crystal samples led to accurate anisotropic thermal parameters, which is relevant for the perception of diffusion paths. The zigzag ...−M(1)−M(2)−... diffusion paths in the NASICON structure have been extensively described in the past, and the thermal parameters of Na(1) and Na(2) picture well the directions of the expected cationic motion.[2,3] As shown in Figure 4a, it is questionable why carriers prefer the O_3 "window 1" to the more accessible and larger "window 2". In fact, all of the oxygens of the latter are strongly involved in Ti−O bonds, which disable the more direct path by strong Ti···Na electrostatic repulsion.

We examined this aspect on the basis of the joint probability density function (JPDF) (Figure 4a), pertinent projections of which are shown in Figure 4b. The JPDF represents the probability to find atoms around their equilibrium positions, which depends on the interatomic interactions. These interactions can be described by pseudopotentials related to the probability of a given diffusion path.[19] This analysis was successfully applied to BIMEVOX and Brownmillerite anionic conductors.[20,21] To our knowledge, this approach is original for NASICON, and the "best" path found was through window 1, for which the activation energy was much lower than the path through window 2 (0.75 vs 1.1 eV; Figure 4b). This absolute value should not be taken too literally but is comparable to the experimental value for $Na_3Sc_2(PO_4)_3$ (E_a = 0.57 eV).

In conclusion, we have solved the full structural model of α-$Na_3Ti_2(PO_4)_3$ on the basis of high-quality single-crystal data, taking into consideration 120° twin domains consecutive to the triclinic (pseudo-monoclinic) symmetry. The cation/vacancy distribution is fully ordered, in contrast to the majority of the models proposed to date. It shows a homogeneous 3D arrangement of vacancies in comparison with the ordered model proposed for α-$Na_3Sc_2(PO_4)_3$ and could represent the ultimate cationic ordering available in the full $Na_3M_2(PO_4)_3$ series, as verified for M = Fe. For M = Ti, the reversible α → γ transition was observed at 85 °C, leading to the standard disordered $R\bar{3}c$ model. The other insight of this work concerns the direct observation of the most probable Na^+ diffusion paths on the basis of accurate crystallographic data using JPDF analysis, which confirmed the zigzag diffusion scheme.

■ ASSOCIATED CONTENT

Supporting Information. Methods and characterization data. This material is available free of charge via the Internet at http://pubs.acs.org.

■ AUTHOR INFORMATION

Corresponding Author
olivier.mentre@ensc-lille.fr

■ ACKNOWLEDGMENT

The FEDER, CNRS, Région Nord Pas-de-Calais and MESR for funding of X-ray diffractometers. P. Roussel and F. Capet for their help with XRD experiments.

■ REFERENCES

(1) Yaroslavtsev, A. B.; Stenima, I. A. *Russ. J. Inorg. Chem.* **2006**, *51*, S97.
(2) Anantharamulu, N.; Rao, K. K.; Rambabu, G.; Kumar, B. V.; Velchuri, R.; Vithal, M. *J. Mater. Sci.* **2011**, *46*, 2821.
(3) Masquelier, C.; Wurm, C.; Rodriguez-Carjaval, J.; Gaubicher, J.; Nazar, L. *Chem. Mater.* **2000**, *12*, 525.
(4) (a) De la Rochère, M.; D'Yvoire, F.; Collin, G.; Comès, R.; Boilot, J. P. *Solid State Ionics* **1983**, *9−10*, 825. (b) D'Yvoire, F.; Pintard-Scrépel, M.; Bretey, E.; De la Rochère, M. *Solid State Ionics* **1983**, *9−10*, 851.
(5) Efrenov, V. A.; Kalinin, V. B. *Kristallografiya* **1978**, *23*, 703.
(6) Sotofte, I.; Fu, D.-C. *Solid State Ionics* **1988**, *26*, 307.
(7) Collin, G.; Comes, R.; Boilot, J. P.; Colomban, P. *J. Phys. Chem. Solids* **1986**, *47*, 843.
(8) Fanjat, N.; Soubeyroux, J. L. *J. Magn. Magn. Mater.* **1992**, *104*, 933.
(9) (a) Delmas, C.; Olazcuaga, R.; Cherkaoui, F.; Brochu, R.; Le Flem, G. *C. R. Acad. Sci. Paris, Ser. C* **1978**, *287*, 169. (b) Beltran Porter, D.; Olazcuaga, R.; Delmas, C.; Cherkaoui, F.; Brochu, R.; Le Flem, G. *Rev. Chim. Miner.* **1980**, *17*, 458.
(10) Delmas, C.; Nadiri, A. *Solid State Ionics* **1988**, *28−30*, 419.
(11) *SAINT: Area-Detector Integration Software*; Siemens Industrial Automation, Inc.: Madison, WI, 1995.
(12) *SADABS: Program for Area-Detector Absorption Correction*; Siemens Industrial Automation, Inc.: Madison, WI, 1996.
(13) Petricek, V.; Dusek, M.; Palatinus, L. *JANA2000: The Crystallographic Computing System*; Institute of Physics: Praha, Czech Republic, 2000.
(14) Pintard-Scrépel, M.; D'Yvoire, F.; Rémy, F. *C. R. Acad. Sci. Paris, Ser. C* **1978**, *286*, 381.
(15) Maximov, B. A.; Bolotina, N. B.; Simonov, V. I. *Acta Crystallogr.* **1994**, *B50*, 261.
(16) Ivanov, Yu. A.; Belokoneva, E. L.; Egorov-Tismenko, Yu. K.; Simonov, N. V. *Dokl. Akad. Nauk SSSR* **1980**, *252*, 1122.
(17) (a) Tamazyan, R. A.; Maksimov, B. A.; Bolotina, N. B.; Novikova, N. E.; Simonov, V. I. *Crystallogr. Rep.* **1994**, *39*, 422. (b) Maximov, B.; Sirota, M.; Werner, S.; Schulz, H. *Acta Crystallogr.* **1999**, *B55*, 259.
(18) Paris, M. A.; Martinez-Juarez, A.; Iglesias, J. E.; Rojo, J. M.; Sanz, J. *Chem. Mater.* **1997**, *9*, 1430.
(19) Bachman, R.; Schulz, H. *Acta Crystallogr.* **1984**, *A40*, 668.
(20) Roussel, P.; Vannier, R. N.; Anne, M.; Nowogrocki, G.; Mairesse, G. *Acta Crystallogr.* **2002**, *A58* (Suppl.), c319.
(21) Rolle, A.; Roussel, P.; Giridharan, N. V.; Suard, E.; Vannier, R. N. *Solid State Ionics* **2008**, *179*, 1986.